

CrystEngComm

Accepted Manuscript



This is an *Accepted Manuscript*, which has been through the Royal Society of Chemistry peer review process and has been accepted for publication.

Accepted Manuscripts are published online shortly after acceptance, before technical editing, formatting and proof reading. Using this free service, authors can make their results available to the community, in citable form, before we publish the edited article. We will replace this *Accepted Manuscript* with the edited and formatted *Advance Article* as soon as it is available.

You can find more information about *Accepted Manuscripts* in the [Information for Authors](#).

Please note that technical editing may introduce minor changes to the text and/or graphics, which may alter content. The journal's standard [Terms & Conditions](#) and the [Ethical guidelines](#) still apply. In no event shall the Royal Society of Chemistry be held responsible for any errors or omissions in this *Accepted Manuscript* or any consequences arising from the use of any information it contains.

HIGHLIGHT

Structural features and applications of Metal-Organic Frameworks containing thiazole- and thiazolidine-based spacers

Cite this: DOI: 10.1039/x0xx00000x

Received 00th January 2012,
Accepted 00th January 2012

DOI: 10.1039/x0xx00000x

www.rsc.org/

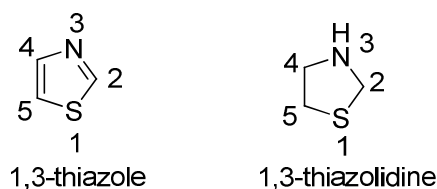
A. Rossin* and G. Giambastiani

This highlight focuses on the analysis and comparison of the network topologies of thiazole- and thiazolidine-containing metal-organic frameworks and coordination polymers, along with the description of their applications in the fields of luminescence, magnetism, CO₂ storage and heterogeneous catalysis.

Introduction

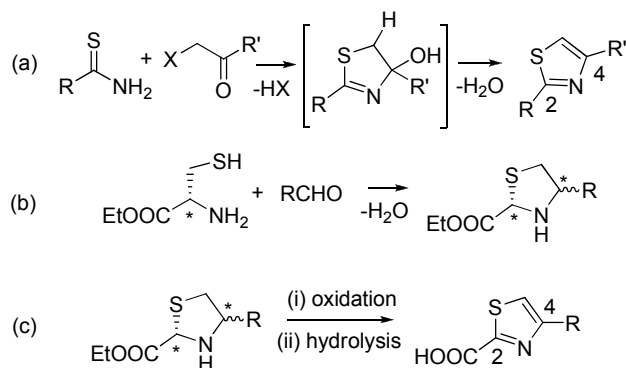
The virtually infinite choice and combination of inorganic nodes and organic linkers for the construction of metal-organic frameworks (MOFs) is the key factor that makes them so successful for their widespread practical exploitation in several fields of contemporary materials science. The creation of MOFs or coordination polymers (CPs) with variable dimensionality (spanning from 1D chains to 2D sheets or 3D scaffolds as constituting parts of the crystal lattice) is normally achieved through the mixing of metal salts and polytopic linkers under solvothermal conditions.¹ In some cases, the metal ions self-assemble into more complex Secondary Building Units (SBUs) as a result of the “harsh” temperature and pressure synthetic conditions (autogenously generated pressure by prolonged reaction heating in a sealed vessel), generating polyatomic clusters at the lattice nodes, like the (Zn₄O)⁶⁺ motif present in the MOF-5 isorecticular series² or the [Zr₆(μ³-O)₄(μ³-OH)₄]¹²⁺ cluster typical of the UiO-66 family.³ In the creation of new MOFs though, the synthetic chemist is mostly spoilt by the choice of the organic spacers, which can be prepared *ad hoc* with a tailor-made approach for a specific application through the introduction on the ligand backbone of functional groups to make them suitable for catalysis,⁴ luminescence,⁵ magnetism⁶ or gas storage and separation.⁷ The typical MOFs ligands belong to the classes of (aliphatic or aromatic) polycarboxylic acids and polydentate N-heterocyclic bases (such as pyridines, imidazoles, pyrazoles and tetrazoles).⁸ Literature examples can also be found where both acids and bases are present together within the same polymer, giving rise to the so-called “mixed-MOFs” (MIXMOFs).⁹ The same definition holds for “homoleptic” frameworks built of more than one chemically distinct spacer, *i.e.* two different carboxylic acids (like UMCM-1¹⁰ or the MIXMOF-5 family¹¹) or two different N-heterocyclic bases (4,4'-bipy/pyrazine,¹² 4,4'-bipy/pyrazolate¹³ or 4,4'-

bipy/imidazolate¹⁴). While N-heterocycles as spacers are ubiquitous, there are fewer examples of MOFs or CPs built with more than one heteroatom type in the heterocyclic core. Besides modifying the electron density distribution within the linker, additional heteroatoms may represent alternative coordination sites for the metal ions employed for the MOF synthesis. The increased overall bond polarization within the cycle is highly desired in gas storage applications; in fact, it has been proved (both theoretically¹⁵ and experimentally¹⁶) that a MOF with increased bond polarity or doped with extra-alkaline metal ions in the lattice has an improved gas adsorption capacity for those gases with a very small dipole moment (H₂, CH₄, CO₂). In addition, the abundance of electron-rich atoms in the linkers increases the number of non-covalent interactions (like hydrogen bonds or π···π stacking) in the solid state, making the material more thermally/chemically stable and creating fascinating supramolecular architectures. N,S-containing heterocycles in particular are intriguing building blocks. The simultaneous presence of a hard (N) and a soft (S) base favours the coordination to both hard and soft metal ions, making the related ligand more versatile for MOFs design. The simplest and most naturally occurring N,S heterocycles are thiazoles and thiazolidines (Scheme 1). Thiazoles and the related thiazolium salts are found in many natural products, like the essential vitamin B1 (also called thiamine). Many thiazoles are flavor compounds (present in the roasted peanuts or cooked beef aromas for example) and possess anti-tumoral activity. They have also shown wide practical applications in materials science; several compounds exhibit fluorescence properties¹⁷ (benzothiazoles are present in luciferines, bioluminescent substances that are produced by fireflies) and have been used for the preparation of organic light-emitting diodes (OLEDs) and semiconductor materials.¹⁸



Scheme 1. Thiazole and thiazolidine heterocycles.

The N atom in the heterocycle can be protonated under acidic conditions ($pK_a = 2.5$). As a donor towards Lewis acidic metal ions, it is less basic than pyridine ($pK_a = 5.2$) but more basic than oxazole ($pK_a = 0.8$), isoxazole ($pK_a = -3$), isothiazole ($pK_a = -0.5$) or 1,3,4-thiadiazole ($pK_a = -4.9$). Thiazoles are commonly obtained through the classical Hantzsch reaction between an α -halocarbonyl compound and a thioamide (Scheme 2a); an alternative approach that consists of a simple condensation between an aldehyde and the naturally occurring amino acid L-cysteine followed by oxidation of the corresponding thiazolidine (Scheme 2b-c)¹⁹ has been optimized by our group for the obtainement of assorted 4-substituted 2-carboxythiazoles and thiazolidines for multi-gram scale preparations (that are necessary when the as-synthesized molecule is the starting material for MOFs syntheses).²⁰



Scheme 2. (a) Hantzsch thiazole synthesis. (b,c) Preparation of 4-substituted thiazolidine- and thiazole-2-carboxylic acids from the naturally occurring L-cysteine.

This highlight will focus on the description from a crystallographic perspective of MOFs/CPs containing thiazoles and thiazolidines within their organic constituents. A brief paragraph dealing with the practical applications of these organic/inorganic hybrid materials in the fields of gas storage, luminescence and magnetism will also be developed at the end of the discussion.

Discussion

1. Thiazole-based MOFs and/or CPs

Table 1 lists all the compounds discussed in this section classifying them by ligand type. The simplest ligand

conceivable is thiazole itself; indeed, simple 1D chains have been obtained through the combination of monodentate κ -N thiazole and metal halides from the first transition series, where the halogen atom acts as a bridge between adjacent metal centers. The resulting polymers have general formula $[MX_2(\kappa$ -N-thiazole) $]_n$ (**1-5**; $M^{II} = Fe, Ni, Co, Cu$; $X = Cl, Br$).²¹ In the solid state, the metal ion has octahedral coordination geometry, where the equatorial positions are occupied by the bridging halides and the axial positions by two thiazole molecules. The network topology calculated with the TOPOS 4.0 software²² is **2C1**, typical of linear 1D chains. The same crystal lattice topology is obtained when using a different bridging anion, like SiF_6^{2-} . The compound $[Cu(\kappa$ -N-thiazole) $](SiF_6)_n$ (**6**) shows a distorted octahedral coordination environment (Jahn-Teller effect) for Cu^{II} , and the equatorial positions are occupied by four monodentate thiazole molecules. Cu-F-Si-F-Cu linear arrangements are present on the axial positions (Fig. 1).²³

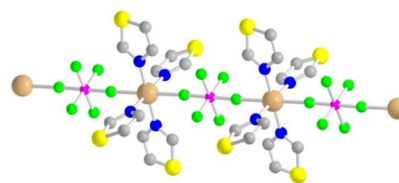


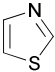
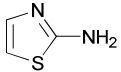
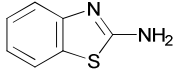
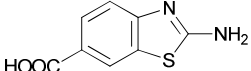
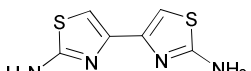
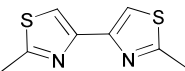
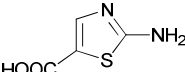
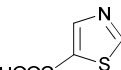
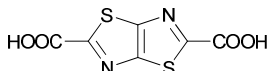
Fig. 1. The 1D chain in the lattice of **6**. Atom color code: gray, C; blue, N; yellow, S; green, F; magenta, Si; copperbrown, Cu. Reproduced with permission from ref. 23.

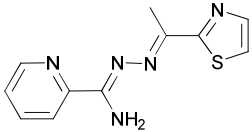
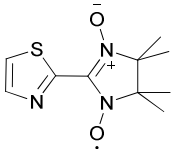
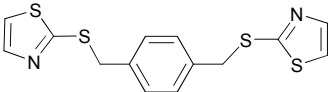
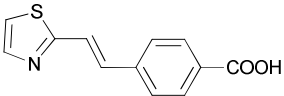
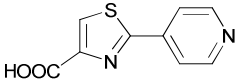
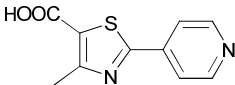
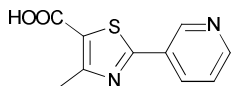
Infinite linear chains in the solid state are obtained with $L = 2$ -aminothiazole and cadmium thiocyanate, in the compound $[Cd(\kappa$ -N-L) $](SCN)_2$ (**7**).²⁴ Two SCN^- ions are bridging adjacent Cd^{II} centers, in an octahedral coordination geometry with a N_4S_2 donor set. 2-aminothiazole is monodentate through the cyclic N atom in an alternate *cis* and *trans* conformation.

Colourless crystals of the linear polymer $[HgCl_2(\kappa$ -N-L) $]_n$ (**8**) are prepared from slow evaporation of water/acetonitrile mixtures of $HgCl_2$ and $L = 2$ -aminobenzothiazole.²⁵ Pairs of bidentate bridging Cl^- anions connect Hg^{II} centers, which are 5-coordinated in a NCl_4 donor set. The coordination geometry is (distorted) trigonal bipyramidal, and the ligand is monodentate through the cyclic N atom. Additional $N-H \cdots Cl$ hydrogen bonding between the hexocyclic amino group and the chloride atoms lead to supramolecular 2D layers in the crystallographic *ab* plane.

The bridging species 2-aminobenzothiazole-6-carboxylate, together with the auxiliary ligand 2,2'-bipyridyl, forms a 1D chain in the presence of Cd^{II} precursors. The resulting compound has minimal formula $[Cd(\mu$ - κ -N: κ -COO-L) $](\kappa^2$ -N,N'-2,2'-bipy) $]$ (**9**).²⁶ The CdN_3O_4 coordination polyhedron is a distorted pentagonal bipyramid with one O and one N atoms on the axial positions. 2,2'-bipyridyl is in a chelating mode. The infinite chain propagates along the [100] Miller direction, through bridging coordination of the carboxylate group and the thiazole N atom. Extensive $N-H \cdots O$ and $N-H \cdots N$ hydrogen bonding engaged by the exocyclic $-NH_2$ groups creates a

Table 1. Thiazole-based organic linkers discussed in this work, along with the related MOFs/CPs formulae and net topology.

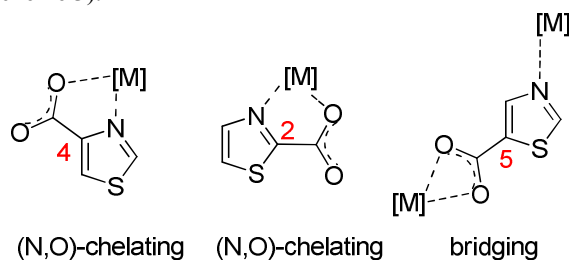
Ligand formula	MOFs/CPs unit formulae	Dimensionality / Net topology	Ref.
 Thiazole	$[\text{FeCl}_2(\text{L})_2]_\infty$ (1) $[\text{FeBr}_2(\text{L})_2]_\infty$ (2) $[\text{NiBr}_2(\text{L})_2]_\infty$ (3) $[\text{CoCl}_2(\text{L})_2]_\infty$ (4) $[\text{CoBr}_2(\text{L})_2]_\infty$ (5) $[\text{CuSiF}_6(\text{L})_4]_\infty$ (6)	1D / 2C1	[21c] [21c] [21b] [21a] [21a] [23]
 2-aminothiazole	$[\text{Cd}(\text{SCN})_2(\text{L})_2]_\infty$ (7)	1D / 2C1	[24]
 2-aminobenzothiazole	$[\text{HgCl}_2(\text{L})_2]_\infty$ (8)	1D / 2C1	[25]
 2-aminobenzothiazole-6-carboxylic acid (HL)	$[\text{Cd}(\text{L})_2(2,2'\text{-bipy})]_\infty$ (9)	1D / 2C1	[26]
 2,2'-diamino-4,4'-bithiazole	$[\text{Mn}(\text{terephthalate})(\text{L})(\text{H}_2\text{O})_2 \cdot 2\text{H}_2\text{O}]_\infty$ (10) $[\text{Pb}(\text{SCN})(\text{NO}_3)(\text{L})]_\infty$ (11)	1D / 2C1	[27] [28]
 2,2'-dimethyl-4,4'-bithiazole	$[\text{CdCl}_2(\text{L})]_\infty$ (12) $[\text{CdBr}_2(\text{L})]_\infty$ (13)	1D / 2C1	[29b] [29a]
 2-aminothiazole-5-carboxylic acid (HL)	$[\text{Cu}(\text{L})_2 \cdot (\text{H}_2\text{O})]_\infty$ (14)	2D / sql	[23]
 Thiazole-5-carboxylic acid (HL)	$[\text{Cu}(\text{L})_2 \cdot 1.5(\text{H}_2\text{O})]_\infty$ (15)	2D / sql	[23]
 Thiazolo[5,4-d]thiazole-2,5-dicarboxylic acid	$[\text{Mn}(\text{L})(\text{H}_2\text{O})_2]_\infty$ (16) $[\text{Co}(\text{L})(\text{H}_2\text{O})_2]_\infty$ (17) $[\text{Cu}(\text{L})(\text{H}_2\text{O})]_\infty$ (18) $[\text{Zn}(\text{L})(\text{H}_2\text{O})_2]_\infty$ (19) $[\text{Ag}_2(\text{L})]_\infty$ (20)	1D / 2C1 1D / 2C1 1D / 2C1 1D / 2C1 3D	[31] [31] [31] [31] [31]

 <p>1-(2-pyridyl)-1-amino-4-methyl-4-thiazolyl-2,3-aza-1,3-butadiene (HL)</p>	$[\text{Zn}_2(\text{L})(\text{N}_3)_3]_\infty$ (21)	3D / snp ($3^6 \cdot 4^4 \cdot 6^6 \cdot 7$)	[32]
 <p>2-(2-thiazole)-4,4,5,5-tetramethyl-4,5-dihydro-1H-imidazolyl-1-oxy-3-oxide</p>	$\{\text{Mn}(\text{L})[\text{N}(\text{CN})_2]_2\}_\infty$ (22)	3D / dia (6^6)	[33]
 <p>2,2'-[1,4-phenylenebis(methylenethio)]bisthiazole</p>	$[\text{Ag}_2(\text{L})(\text{NO}_3)_2 \cdot \text{EtOH}]_\infty$ (23)	2D / ($3^9 \cdot 4^{18} \cdot 5$)	[34]
 <p>(E)-4-(2-thiazolyl)ethenylbenzoic acid (HL)</p>	$[\text{Cd}_2(\text{L})_4(\text{H}_2\text{O})]_\infty$ (24)	2D / tts ($3^3 \cdot 4^5 \cdot 5^4$)	[35]
 <p>2-(4-pyridyl)-thiazole-4-carboxylic acid (HL)</p>	$[\text{Cu}_3(\text{L})_6 \cdot (\text{H}_2\text{O})_{14}]_\infty$ (25) $[\text{Zn}(\text{F})(\text{L}) \cdot \text{H}_2\text{O}]_\infty$ (26) $[\text{Zn}(\text{L})_2 \cdot (\text{H}_2\text{O})_{4/3}]_\infty$ (27) $[\text{Ag}(\text{L}) \cdot \text{H}_2\text{O}]_\infty$ (28) $[\text{Co}_3(\text{L})_6 \cdot (\text{H}_2\text{O})_8]_\infty$ (29) $[\text{Co}_3(\text{L})_2(\text{V}_4\text{O}_{12})(\text{H}_2\text{O})_4]_\infty$ (30) $[\text{Cd}(\text{I})(\text{L})(\text{H}_2\text{O}) \cdot \text{H}_2\text{O}]_\infty$ (31) $[\text{Cd}(\text{L})_2(\text{H}_2\text{O})_4]$ (32) $[\text{Pb}(\text{L})_2]_\infty$ (33) $[\text{Pb}_2(\text{L})_3(\text{NO}_3)]_\infty$ (34)	3D / ($4^2 \cdot 6^2 \cdot 8^2$)($4 \cdot 6^4 \cdot 8$) 3D 2D / sql ($4^4 \cdot 6^2$) 3D / ($3^{12} \cdot 4^{20} \cdot 5^{11} \cdot 6^2$) 3D 3D 3D 1D 0D 2D 1D	[36] [37] [37] [38] [38] [38] [38] [38] [38] [39] [39]
 <p>2-(4-pyridyl)-4-methylthiazole-5-carboxylic acid (HL)</p>	$[\text{Cd}(\text{L})_2(\text{H}_2\text{O})_4(\text{DMF})]_\infty$ (35) $[\text{Mn}(\text{L})_2(\text{H}_2\text{O})_3(\text{DMF})]_\infty$ (36)	3D / bcu ($4^{24} \cdot 6^4$) 3D / bcu ($4^{24} \cdot 6^4$)	[40] [40]
 <p>2-(3-pyridyl)-4-methylthiazole-5-carboxylic acid (HL)</p>	$[\text{Ni}(\text{L})_2(\text{H}_2\text{O})_4]_\infty$ (37-38) $[\text{Zn}(\text{L})_2(\text{H}_2\text{O})]_\infty$ (39) $[\text{Cu}(\text{L})_2(\text{H}_2\text{O})]_\infty$ (40)	2D 2D 2D	[41] [41] [41]

supramolecular 3D net. Additional stabilizing $\pi \cdots \pi$ interactions between the thiazole and bipy rings are also present. Chelating ligands ($\kappa^2\text{-N,N'}$, analogous to 2,2'-bipy as a coordination

mode) derived from 4,4'-bithiazole and bearing different substituents on the 2 and 2' positions have been exploited for the synthesis of 1D CPs having the same network topology.

The chain propagation in the lattice is guaranteed by the presence of an extra bridging ligand anionic in nature, like the terephthalate anion in $[\text{Mn}(\text{terephthalate})(2,2'\text{-diamino-4,4'\text{-bithiazole})(\text{H}_2\text{O})_2 \cdot 2\text{H}_2\text{O}]_\infty$ (**10**),²⁷ the thiocyanate/nitrate anions in $[\text{Pb}(\text{SCN})(\text{NO}_3)(2,2'\text{-diamino-4,4'\text{-bithiazole})]_\infty$ (**11**)²⁸ or simple halides as in $[\text{CdX}_2(2,2'\text{-dimethyl-4,4'\text{-bithiazole})]_\infty$ (**12-13**; X = Cl, Br).²⁹ With simple thiazole carboxylic acid as a spacer, moving the $-\text{COOH}$ group from the 2-/4- to the 5-position of the heterocyclic ring leads to bridging rather than chelating ligands, more suitable for MOFs synthesis (Scheme 3).³⁰



Scheme 3. The different coordination modes of thiazolecarboxylic acid regioisomers.

Indeed, 2D coordination networks have been obtained with suitable Cu^{II} precursors under solvothermal conditions. The compounds $\{\text{Cu}[\mu-(\kappa\text{-}N:\kappa\text{-}COO)\text{-L}]_2 \cdot (\text{H}_2\text{O})\}_\infty$ (**14**; HL = 2-aminothiazole-5-carboxylic acid) and $\{\text{Cu}[\mu-(\kappa\text{-}N:\kappa\text{-}COO)\text{-L}]_2 \cdot 1.5 (\text{H}_2\text{O})\}_\infty$ (**15**; HL = thiazole-5-carboxylic acid) belong to the **sql** ($4^4\text{-}6^2$) network topology, revealing a 2D polymeric structure.²³ In the lattice of **14**, undulated sheets extend along the [001] Miller direction, kept together by the extensive sheet-sheet and water-sheet $\text{N-H}\cdots\text{O}$ hydrogen bonding engaged by the exocyclic $-\text{NH}_2$ substituents on the ligand with either adjacent carboxylate groups or with crystallization water molecules. In **15**, the 2D regular grid along the [101] Miller direction is more planar, and the ordered stacking of the bidimensional sheets along the a axis generates supramolecular 3D channels (Fig. 2).

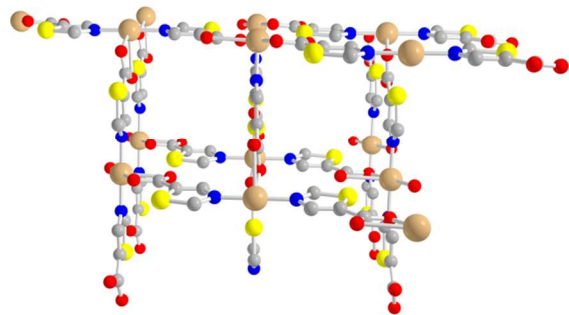


Fig. 2. View of the 3D supramolecular channels in the lattice of **15**. Atom color code: gray, C; blue, N; yellow, S; red, O; copperbrown, Cu. Reproduced with permission from ref. 23.

Dense 1D CPs have been obtained with the symmetrical spacer thiazolo[5,4-d]thiazole-2,5-dicarboxylic acid combined with transition metal ions from the first series, under hydrothermal conditions. Within these compounds, of general formula $[\text{M}(\text{L})(\text{H}_2\text{O})_x]_\infty$ (**16-19**; $\text{M}^{\text{II}} = \text{Mn, Co, Cu, Zn}$; $x = 1, 2$),³¹ the ligand adopts a preferential (*N,O*)-chelating rather than the (*O,O'*)-bridging mode, as observed in analogous cases where the carboxylic functional group occupies an α -position with respect to the heterocyclic N (*i.e.* either on the C-2 or on the C-4 position). The metal ions are octahedrally coordinated; water molecules complete the N_2O_4 coordination sphere, and they engage into hydrogen-bonding interactions with the carboxylate groups of the adjacent chains in the lattice. A genuine 3D framework is instead obtained with silver(I): $[\text{Ag}_2(\text{L})]_\infty$ (**20**). The coordination geometry at the metal centre is diagonal (severe distortion from linearity is observed), with extra-interactions with the S atoms of the ligands.

Crystals of the compound $[\text{Zn}(\text{HL})(\text{N}_3)_3]_\infty$ (**21**) have been obtained through slow diffusion of methanolic solutions of Zn^{II} perchlorate hydrate, the ligand HL = 1-(2-pyridyl)-1-amino-4-methyl-4-thiazolyl-2,3-aza-1,3-butadiene (an open chain diazine Schiff-base) and sodium azide in a H-shaped tube.³² The ligand is anionic and pentadentate, bridging adjacent metal ions in a $\eta^2:\eta^3$ mode. The thiazole fragment of the spacer is coordinated through its N atom. In the asymmetric unit, there are two non-equivalent Zn^{II} ions, one with a pseudo-octahedral geometry and the other with a distorted square pyramidal ligand arrangement. Additional end-on azido bridges form $\text{Zn}_2(\text{N}_3)_2$ four-membered rings that complete the tridimensional connection, generating a ($3^6\text{-}4^4\text{-}6^6\text{-}7$) **snp** net topology (Fig. 3).

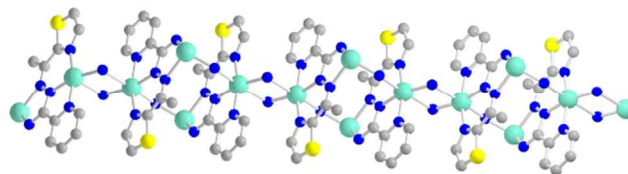


Fig. 3. View of the 3D lattice of **21**. Atom color code: gray, C; blue, N; yellow, S; aquamarine, Zn. $\text{Zn}_2(\text{N}_3)_2$ four-membered rings simplified for clarity. Adapted from ref. 32.

The manganese(II) nitronyl-nitroxide MOF $\{\text{Mn}(\text{L})[\text{N}(\text{CN})_2]_2\}_\infty$ (**22**) has been prepared with the Ullman-type radical L = 2-(2-thiazole)-4,4,5,5-tetramethyl-4,5-dihydro-1H-imidazolyl-1-oxy-3-oxide.³³ The dicyanoamide $[\text{N}(\text{CN})_2]^-$ ion shows long-range magnetic ordering properties, and in this case it has also been exploited as a bridging ligand to build the 3D framework around the Mn^{II} ions in an octahedral coordination environment. The radical-ion adopts a chelating bonding mode through one of its N–O bonds and the thiazole N-atom. The resulting framework has **dia** (6^6) topology.

Reaction between the thioether compound L = 2,2'-[1,4-phenylenebis(methylenethio)]bisthiazole and silver nitrate led to the 2D polymer $[\text{Ag}_2(\text{L})(\text{NO}_3)_2 \cdot \text{EtOH}]_\infty$ (**23**).³⁴ In the

lattice, the silver(I) ion is in a tetrahedral coordination environment, and the bridging ligand is in a (*N,S*)-chelating fashion through the thiazole N-atoms and the S atoms coming from the thioether groups. The resulting zigzag chain is propagating along the *b* axis; the nitrate anions are also bridging Ag^I centers coming from adjacent chains, linking them together to form a 2D brick network along the [001] direction with (3⁹·4¹⁸·5) topology. Weak C–H···O hydrogen bonds between the nitrate oxygen atoms and the thiazole C–H bonds are also present.

In situ hydrolysis of a nitrile compound produces the corresponding carboxylate ion during the synthesis of the Cd^{II} coordination polymer [Cd₂(L)₄(H₂O)]_∞ [**24**; L = (*E*)-4-(2-thiazolyl)ethenylbenzoate] in methanol/water binary mixtures under solvothermal conditions.³⁵ The metal SBU is the “paddle-wheel” dimer of Cd₂L₄ type, analogous to the Zn₂L₄ one found in many Zn^{II} MOFs.⁸ The dimers are kept together by four carboxylate bridges (plus one bridging *aquo* ligand), and each Cd₂ dimer is linked to the others via the thiazole N-atom coordination to the vacant coordination position of the octahedral Cd^{II} ions. This ligand arrangement forms a 2D sheet on the crystallographic *ab* plane. The resulting network topology is **tts** (3³·4⁵·5⁴).

The multidentate ligand 2-(4-pyridyl)-thiazole-4-carboxylic acid has been widely exploited for the design of MOFs and CPs of assorted dimensionality. Its ability at acting as a bridging spacer comes from the co-existence of a chelating (*N,O*)-thiazole/COO[−] group at one edge and a terminal pyridine at the opposite edge. The chelating group is not exactly opposite to the terminal pyridine, but they are rather perpendicular to each other. The geometrical constraint forces the ligand to behave as a *bent* (rather than a linear) spacer. This feature generates fascinating multidimensional arrangements in the solid state when combined with transition metal ions.

A 3D net with moganite (4²·6²·8²)(4·6⁴·8)₂ topology has been obtained with Cu^{II}: [Cu₃(L)₆ · (H₂O)₁₄]_∞ (**25**).³⁶ Copper atoms are in a distorted octahedral environment, with a N₄O₂ donor set. The MOF accommodates 14 water molecules per formula unit within channels that extend along the [101] direction. Zinc-containing compounds of unit formula [Zn(F)(L) · H₂O]_∞ (**26**) and [Zn(L)₂ · (H₂O)_{4/3}]_∞ (**27**) have been prepared under similar reaction conditions.³⁷ Both are two-dimensional CPs. In **26**, the Zn^{II} ion is in an octahedral coordination environment, bound to two fluorine atoms on the axial positions, while one water molecule, a chelating carboxylate and the N atom coming from pyridine lie on the equatorial plane. The organic ligand creates infinite chains that are assembled together by F–Zn–F transversal linkages (fluoride anions are in a bridging mode). The resulting extended sheets are hydrogen-bonded to parallel sheets, to form a supramolecular 3D structure. In the homoleptic Zn^{II} compound **27**, the metal ion adopts a trigonal bipyramidal coordination geometry, in a N₂O₃ donor set. The axial positions are occupied by the thiazole N-atoms; one ligand molecule is in a (*N,O*)-chelating coordination mode, while the other is terminally bound to the metal through its –COO[−] group. The resulting

network is made of corrugated 2D sheets [**sql** (4⁴·6²) topology], and the crystallization water molecules lie in between.

Silver gives the [Ag(L) · H₂O]_∞ MOF (**28**).³⁷ It is a chiral 3D polymer (it crystallizes in the chiral *P2₁2₁2₁* space group), where the metal ion is in a distorted tetrahedral N₂O₂ coordination environment. Channels along the [100] direction are filled with water molecules (Fig. 4). The network topology is (3¹²·4²⁰·5¹¹·6²).

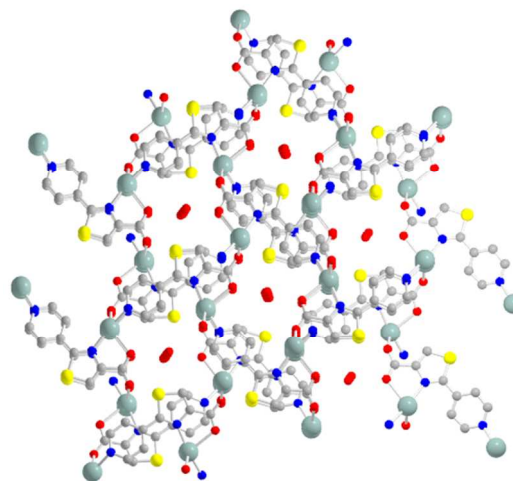


Fig. 4. View along the [100] direction of the 3D lattice of **28**. Atom color code: gray, C; blue, N; yellow, S; red, O; light blue, Ag. Within the channels, crystallization water molecules can be clearly seen. Adapted from ref. 37, Copyright (2006), with permission of Elsevier.

Additional polymeric materials are obtained with cobalt or cadmium ions. In [Co₃(L)₆ · (H₂O)₈]_∞ (**29**), 3D scaffolds are formed by the bridging ligand in a (*N,O*)-chelating/*N*(py)-unidentate mode.³⁸ Channels along the [101] direction contain the crystallization water molecules; the two crystallographically independent Co^{II} centers have octahedral coordination geometry, with N₃O₃ and N₄O₂ donor sets, respectively. When a mixture of cobalt nitrate and ammonium vanadate is used as the inorganic starting material, the compound [Co₃(L)₂(V₄O₁₂)(H₂O)₄]_∞ (**30**) is the final product obtained under hydrothermal conditions.³⁸ This framework contains interlinked layers of 1D strands of two distinct types, purely inorganic [made of Co(H₂O)₄(V₄O₁₂) units, Fig. 5a] and metal-organic [Co₂(L)₂ units, Fig. 5b] in nature. The connection between the two layer types is ensured by O–H···O hydrogen bonding between the aquo ligands and the uncoordinated carboxylate oxygen.

[Cd(L)(H₂O) · H₂O]_∞ (**31**) consists of infinite 1D chains kept together by an extensive hydrogen bonding network.³⁸ The infinite chains propagate along the [01-1] direction and are built from the octahedrally coordinated cadmium(II) centers.

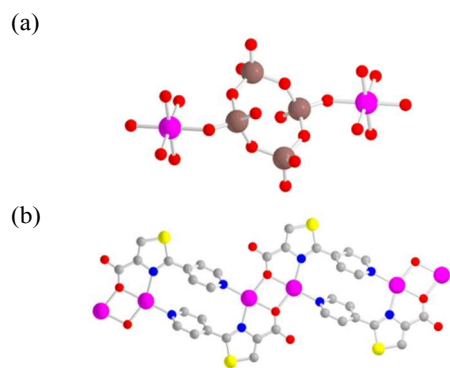


Fig. 5. View of the two distinct interwoven chains in the lattice of **30**: (a) the inorganic $\text{Co}(\text{H}_2\text{O})_4(\text{V}_4\text{O}_{12})$ units, extending along the [0-11] Miller direction. (b) the $\text{Co}_2(\text{L})_2$ units, along the [001] Miller direction (the vanadate oxygen atoms on the axial Co^{II} coordination sites have been omitted for clarity). Atom color code: gray, C; blue, N; yellow, S; red, O; dark brown, V; magenta, Co. Adapted from ref. 38, Copyright (2008), with permission of Elsevier.

The ligand is bridging in the usual (*N,O*)-chelating/*N*(py) unidentate mode. Finally, the 0D molecular complex $[\text{Cd}(\text{L})_2(\text{H}_2\text{O})_4]$ (**32**) is obtained after a slow evaporation of a methanol/water mixture of cadmium(II) acetate, the ligand and NaOH.³⁸ In this case, the abundance of (stabilizing) hydrogen bonding interactions that can be switched on by a free $-\text{COO}^-$ group prevails on the tendency to bridge adjacent metal ions. As a result, a discrete coordination compound rather than a polymer is the preferred product.

The same ligand can be found in the lead(II) species of general formula $[\text{Pb}(\text{L})_2]_\infty$ (**33**, 2D layers) and $[\text{Pb}_2(\text{L})_3(\text{NO}_3)]_\infty$ (**34**, 1D chains), respectively.³⁹ In **33**, the thiazole N-atom is not coordinated, and the ligand is bridging in a (*O,O'*)-chelate/*N*(py)-unidentate fashion; the Pb^{II} ion shows an octahedral coordination geometry. On the contrary, in **34** the thiazole N-atom is engaged into the typical (*N,O*)-chelating coordination mode.

Isomeric variations of the aforementioned ligand have also been exploited for the construction of MOFs. One modification is related to a $-\text{COO}^-$ group shift from the 4- to the 5-position. Another viable option is the modification of the position of the coordinating N on the pyridine fragment, passing from the 4-pyridyl to the 3-pyridyl substituent.

2-(4-pyridyl)-4-methylthiazole-5-carboxylic acid is present within two isostructural 3D frameworks of manganese(II) and cadmium(II) showing permanent porosity: $[\text{Cd}(\text{L})_2(\text{H}_2\text{O})_4(\text{DMF})]_\infty$ (**35**) and $[\text{Mn}(\text{L})_2(\text{H}_2\text{O})_3(\text{DMF})]_\infty$ (**36**; DMF = N,N-dimethylformamide, Fig. 6).⁴⁰ While the Cd^{II} ion is seven-coordinated (pentagonal bipyramidal geometry), the Mn^{II} ion is six-coordinated (octahedral), probably because of the smaller size with respect to Cd^{II} . In both polymers, the ligand is bridging through a (*O,O'*)-chelate/*N*(py)-unidentate mode. Chelation with the N-atom of the thiazole ring is prevented when the carboxylate function is in 5-position. If the

dimeric $\text{M}_2(\text{COO})_4$ clusters are considered as a node, the network topology is **bcu** ($4^{24} \cdot 6^4$).

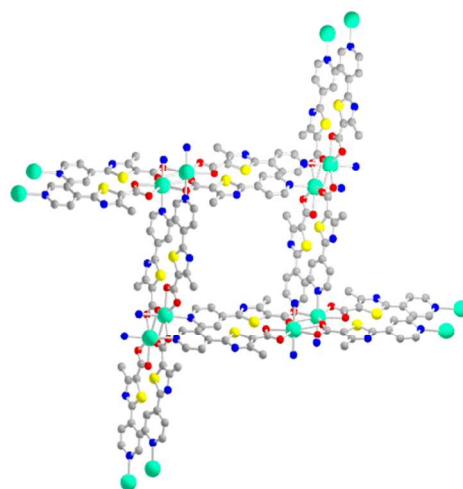
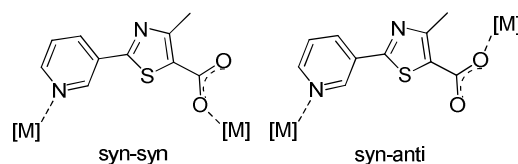


Fig. 6. View of the 3D network of **35**. Atom color code: gray, C; blue, N; yellow, S; red, O; light green, Cd. Adapted from Ref. 40 with permission from the Centre National de la Recherche Scientifique (CNRS) and The Royal Society of Chemistry.

2-(3-pyridyl)-4-methylthiazole-5-carboxylic acid has been assembled with a variety of metal ions from the 3d series.⁴¹ Two conformational polymorphs with the same formula unit $[\text{Ni}(\text{L})_2(\text{H}_2\text{O})_4]_\infty$ (**37-38**) are obtained by changing the metal salt used for the synthesis (either nickel(II) nitrate hydrate or acetate hydrate). Both compounds are two-dimensional grids, where the Ni^{II} centers are in an octahedral coordination geometry, with a N_2O_4 donor set. The four O atoms around the metal come from two *aquo* ligands and two monodentate carboxylates, while the N-atoms come from the pyridyl fragment. The ligand is in a *syn-syn* coordination mode in **37**, and in a *syn-anti* conformation in **38** (Scheme 4). Since the only difference is the counterion used for the synthesis, it seems that, although no anions are included in the final polymer, they may act as templates and play a dominant role during the hydrothermal crystal assembly.



Scheme 4. The different coordination modes of 2-(3-pyridyl)-4-methylthiazole-5-carboxylic acid in MOFs **37** and **38**.

The Zn^{II} and Cu^{II} derivatives are isostructural: $[\text{M}(\text{L})_2(\text{H}_2\text{O})]_\infty$ (**39-40**; $\text{M}^{\text{II}} = \text{Zn}, \text{Cu}$). They are 2D corrugated frameworks, with the metal ion surrounded by an *aquo* ligand and four ligands in a *N*(py)/*O*(carboxylate, unidentate) bridging mode. As usual, an extended hydrogen bonding network among the numerous polar bonds present in the structure keeps the layers interconnected to each other.

2. Thiazolidine-based MOFs and/or CPs

The saturated version of thiazole, thiazolidine, has been used for MOFs synthesis in a few cases. The presence of optically active carbon atoms in the ligand backbone adds further levels of complexity to the rational design of the related hybrid material. When working with optically pure spacers, the final MOF/CP obtained from these building blocks generally maintain the same chiral nature as their constituting ligands. In addition, new applications in scientific contexts where chirality is an added value can be envisaged (*vide infra*). Table 2 collects the ligand structures discussed in this section, along with the related MOFs/CPs.

A 3D MOF built with thiazolidine-2-thione and silver(I) has been prepared through slow solvent diffusion at ambient temperature: $[\text{Ag}_4(\text{L})_4(\text{HL})_2]_\infty$ (**41**).⁴² The tetranuclear $\text{Ag}_4(\text{L})_4$ cluster is self-assembled during the crystal formation; each cluster is then connected to the others *via* (*S,N*)- or *S*-bridging coordination of L. The sulphur atom involved in coordination is always the exocyclic one (from the thione moiety). The resulting network topology is $(3^7 \cdot 4^3)(3^8 \cdot 4 \cdot 9^{12})$.

Homochiral helical CPs have been obtained through the combination of L-thioprolinone (*R*-thiazolidine-4-carboxylic acid) and metals from the first transition series.⁴³ All of them have the same formula unit $[\text{M}(\text{L})_2]_\infty$ (**42-44**), but while $\text{M}^{\text{II}} = \text{Zn}$ gives a 1D polymer made of right-handed helical chains with pentacoordinated Zn^{II} ions, $\text{M}^{\text{II}} = \text{Cd}, \text{Ni}$ form a 2D homochiral framework with **sql** ($4^4 \cdot 6^2$) topology containing right-handed (Cd) or left-handed (Ni) chains, respectively. In these structures, the ligand is chelating the metal centers through its carboxylate group and the cyclic N atom, in the same manner as that observed for the aromatic analogue thiazole-4-carboxylic acid. The spatial arrangement is more “distorted” than that of thiazole though, since the ring is not planar and it adopts the typical “envelope” conformation of penta-atomic aliphatic rings (*i.e.* cyclopentane).

Thiazolidine-2,4-dicarboxylic acid has been exploited for the synthesis of a number of MOFs containing cobalt and nickel. The as-synthesized materials are optically pure, despite the use of a racemic mixture of the (*R,S*) and (*R,R*) ligand diastereoisomers. Spontaneous resolution occurs, and chirality is introduced in the final MOFs either through a temperature-directed process or through an external driving force such as solvent or additives. An example of temperature-directed structural recurrence is ~~An interesting temperature dependent conformational change has been recorded in~~ the synthesis of the two polymers of molecular formulae ~~isomeric forms~~ $[\text{Co}(\text{L})(\text{H}_2\text{O})_2 \cdot \text{H}_2\text{O}]_\infty$ (**45**) and $[\text{Co}(\text{L})(\text{H}_2\text{O}) \cdot 0.5\text{H}_2\text{O}]_\infty$ (**46**).⁴⁴ At ambient temperature, the preferred ligand conformation is the (*R,S*)-*transoid* one, while at higher (353 K) or lower (278 K) temperature the (*R,R*)-*cisoid* conformation is the one found in the final polymer. As a consequence, in the former case a 1D helical chain crystallizing in the $P2_1$ space group is isolated, while in the latter case a chiral 3D framework of $(3^3 \cdot 5^5 \cdot 6^6 \cdot 7)$

topology showing permanent porosity and crystallizing in the $P4_1$ space group is the final reaction outcome. In **46**, two different channels are alternating within the crystal lattice, one hydrophilic (with the exposed *aquo* ligands forming hydrogen bonding with the crystallization water molecules within the channels) and the other hydrophobic (with exposed S atoms from the spacer, Fig. 7). Circular Dichroism measurements have proved that the chiral information in the (enantiomerically pure) ligand is preserved in the corresponding MOF.

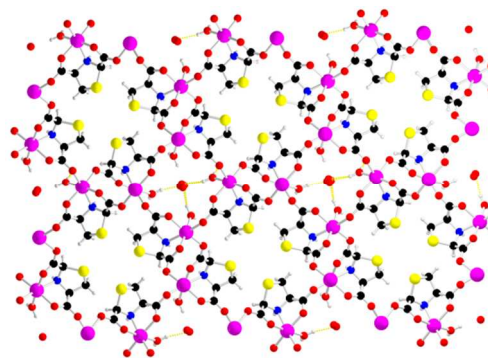


Fig. 7. View of the 3D lattice of **46**. Atom color code: black, C; blue, N; yellow, S; red, O; magenta, Co. Reproduced with permission from ref. 44b.

Additives can also induce the same phenomenon. The nickel(II) compounds $[\text{Ni}(\text{L})(\text{H}_2\text{O})_2 \cdot \text{H}_2\text{O}]_\infty$ (**47**) and $[\text{Ni}(\text{L})(\text{H}_2\text{O}) \cdot 0.5\text{H}_2\text{O}]_\infty$ (**48**)⁴⁵ are isostructural with **45** and **46**, respectively. In the presence of polyvinylpyrrolidone (PVP) as a surfactant, a preferential formation of **47** occurs, at both ambient and high temperature (353 K), thus revealing the influence of surfactants on the reaction course. In this specific case, the ability of PVP at engaging into hydrogen bonds with the polar groups present in the ligand has been invoked as the key factor that influences the reaction outcome. The effect of PVP is even stronger than that of temperature.

3. Applications of thiazole- and thiazolidine-based MOFs

3.1. Luminescence

Luminescent properties are mostly related to the intraligand $\pi \rightarrow \pi^*$ or $n \rightarrow \pi^*$ electronic transitions, albeit in a very few cases a metal-to-ligand (MLCT) or a ligand-to-metal (LMCT) charge transfer has been observed. In compound **8**, a strong emission band at $\lambda = 361$ nm is ascribed to the $\pi \rightarrow \pi^*$ transition of the 2-aminobenzothiazole spacer.²⁵ In the L-thioprolinone derivatives **42** and **43**, blue fluorescent emission peaks at $\lambda = 458$ and 452 nm are recorded respectively, with a strong red shift with respect to the free ligand, whose emission is centered at $\lambda = 398$ nm.⁴³ Since Zn^{II} or Cd^{II} are notoriously difficult to be oxidized or reduced because of their stable d^{10} electronic configuration, the observed MOFs emissions are reasonably due to the proline internal transitions (modified by its metal coordination). The red shift is ascribed to the chelation to the metal ions, which

increases the rigidity and the localization of electrons on the organic rather than the inorganic MOF component.

Table 2. Thiazolidine-based organic linkers discussed in this work, along with the related MOFs/CPs formulae and net topology.

Ligand formula	MOFs/CPs unit formulae	Dimensionality / Net topology	Ref.
thiazolidine-2-thione (L)	$[\text{Ag}_4(\text{L})_4(\text{HL})_2]_\infty$ (41)	3D / $(3^7 \cdot 4^3)(3^8 \cdot 4 \cdot 9^{12})$	[42]
L-thioproline (<i>R</i> -thiazolidine-4-carboxylic acid) (HL)	$[\text{Zn}(\text{L})_2]_\infty$ (42)	1D	[43]
	$[\text{Cd}(\text{L})_2]_\infty$ (43)	2D / sql ($4^4 \cdot 6^2$)	[43]
	$[\text{Ni}(\text{L})_2]_\infty$ (44)	2D / sql ($4^4 \cdot 6^2$)	[43]
Thiazolidine-2,4-dicarboxylic acid (H_2L)	$[\text{Co}(\text{L})(\text{H}_2\text{O})_2 \cdot \text{H}_2\text{O}]_\infty$ (45)	1D	[44a]
	$[\text{Co}(\text{L})(\text{H}_2\text{O}) \cdot 0.5\text{H}_2\text{O}]_\infty$ (46)	3D / $(3^3 \cdot 5^5 \cdot 6^6 \cdot 7)$	[44b]
	$[\text{Ni}(\text{L})(\text{H}_2\text{O})_2 \cdot \text{H}_2\text{O}]_\infty$ (47)	1D	[45]
	$[\text{Ni}(\text{L})(\text{H}_2\text{O}) \cdot 0.5\text{H}_2\text{O}]_\infty$ (48)	3D / $(3^3 \cdot 5^5 \cdot 6^6 \cdot 7)$	[45]

3.2. Magnetism

When a paramagnetic metal ion is the inorganic constituting part of the MOF, the existence of ferromagnetic or antiferromagnetic interactions between the metal centers has been assessed in a number of cases. Room temperature magnetic susceptibility of **1** is consistent with a high-spin Fe^{II} ion, with the possibility of intrachain magnetic superexchange occurring *via* the dihalide bridges.²¹ In polymers **4** and **5**, magnetization measurements at 5 K reveal a metamagnetic transition between antiferromagnetic and ferromagnetic states.²¹ As for **1**, ferromagnetic interactions between the Co^{II} centers are present along the direction of the 1D chain, because of the halide bridges. In species **22**, the strong antiferromagnetic interactions present are switched on more by the Mn-radical than by the Mn-dicyanoamide contacts.³³ In **36**, antiferromagnetic interactions within the dimeric Mn_2L_4 units are present, over the 2-300 K temperature range.⁴⁰

3.3. CO_2 storage

The 2D polymer **15** has been exploited for CO_2 adsorption under ambient temperature and pressure conditions ($T = 298 \text{ K}$, $p_{\text{CO}_2} = 1 \text{ atm}$).²³ Despite its low BET surface area (only $15 \text{ m}^2/\text{g}$, measured through N_2 physisorption at $T = 77 \text{ K}$), the material is mesoporous, and it shows a remarkable CO_2 uptake of 9.0 wt.% (Fig. 8). This value is comparable with those of other Cu-based MOFs with a much higher BET specific surface area. The selectivity for CO_2 over N_2 is also guaranteed by a direct comparison of the gas weight percentage adsorbed at a given absolute pressure (from the pressure-composition plots). This

selectivity makes the material promising for applications in carbon dioxide post-combustion capture in industrial processes.

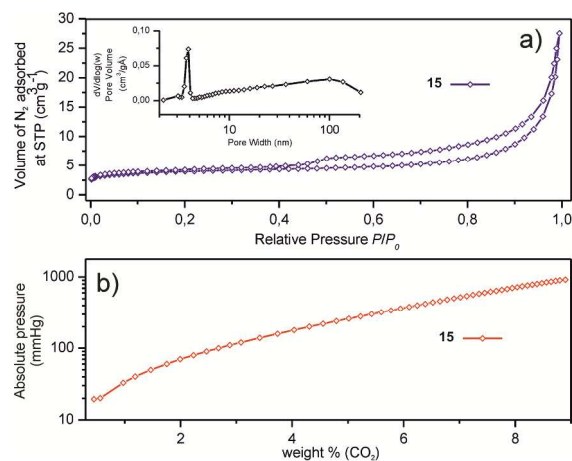


Fig. 8. (a) N_2 adsorption isotherm of **15** at $T = 77 \text{ K}$ and (inset) related pore size distribution (BJH model, Harkins-Jura approximation). (b) Pressure-composition plot for CO_2 physisorption on **15** at $T = 303 \text{ K}$, $p_{\text{CO}_2} \text{ max.} = 920 \text{ torr}$. Reproduced with permission from ref. 23.

The Cd^{II} MOF **35** has been tested for CO_2 physisorption at different temperatures ($T = 273, 288$ and 298 K) and ambient pressure.⁴⁰ The adsorption isotherms are of type-I, typical of a microporous material. The maximum uptake at ambient conditions equals 5.8 wt.%. **35** has been found to be selective

for CO₂ sorption over a wide range of gases (CH₄, N₂, O₂, H₂ and CO). The high affinity of the material for CO₂ has also been confirmed by the experimental measurement of the isosteric heat of adsorption, which is around 21.5 kJ mol⁻¹, holding potential for *gas mixtures separation/purification* applications of industrial relevance.

The thiazolidine-based MOF **45** has also been exploited for CO₂ capture; for this material (pre-activated after water removal), the maximum gas uptake at T = 273 K and p_{CO₂} = 1 atm equals 4.7 wt.%.^{44b} The isotherm though does not show any plateau at p = 1 atm, this suggesting that this value could be significantly improved at higher pressures.

3.4. Heterogeneous catalysis

The enantiomerically pure Co^{II} MOF **45** has been exploited in alkenes oxidation under aerobic (O₂ as oxidant) and anaerobic (*tert*-butyl hydroperoxide as oxidant) conditions.⁴⁶ Different alkenes have been employed (cyclohexene, Z-cyclooctene, 1-octene), and different chemoselectivity is observed, being both substrate- and oxidant-dependent. A moderate enantioselectivity is also obtained in the case of pro-chiral precursors, revealing the chiral induction ability of the optically pure metal environment. Among the various olefins considered, cyclohexene is the most efficiently oxidized substrate. During its anaerobic oxidation, a 100 % selectivity towards the chiral *tert*-butyl-2-cyclohexenyl-1-peroxide product has been achieved, albeit with a moderate conversion (at t = 24 h). The highest conversion (37 % after 24 h) reported to date for a Co-MOF catalyzed cyclohexene oxidation (but a lower selectivity) is achieved under aerobic conditions, leading to the α,β-unsaturated ketone 2-cyclohexenone as the main product. As a complement to the experimental work, a DFT computational analysis of O₂ interaction with the exposed metal sites in **45** (after water removal) was performed. The optimized structures, the calculated atomic charges and the spin state are consistent with the η¹-superoxo nature of bound O₂ (Fig. 9).

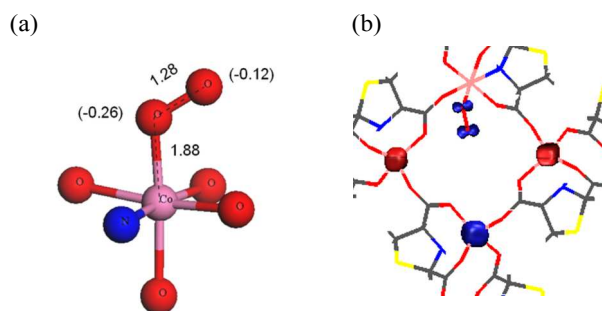


Fig. 9. DFT-optimized geometry of one O₂ molecule/cell adsorbed by **45**. (a) The coordination environment of the cobalt center after O₂ adsorption. The internuclear O-O and Co-O distances (Å) are reported. Atomic charges transferred to O atoms are reported in parenthesis. (b) The unpaired spin density surfaces in **45** after O₂ adsorption. Reprinted with permission from ref. 46. Copyright (2014), American Chemical Society.

Summary

A comprehensive survey of thiazole- and thiazolidine-containing MOFs has been presented here. Almost fifty compounds have appeared in the literature since the first examples in 1998. The wide variety of network topologies and dimensionality that is recorded for this class of materials stems from the multidentate nature of the organic linkers bearing N,S-containing heterocycles with more than one coordination site within the linker core. The abundance of polar C–N, C–S, N–S bonds in the lattice facilitates the occurrence of stabilizing weak interactions and represents an added value for future practical applications in (polar) gas storage and separation *via* selective physisorption. Last but not least, the heterocycles luminescent properties can be exploited in photocatalytic organic transformations. There is still plenty to discover in this field of MOFs science!

Acknowledgements

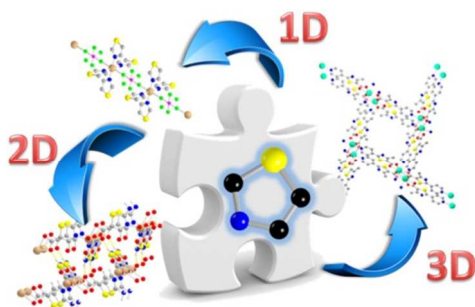
Our research on thiazole- and thiazolidine-containing MOFs has been supported by grants from the FIRENZE HYDROLAB 2 project supported by ECRF, the Premiale project “Energia da fonti rinnovabili” 2010-2012 of the Italian National Research Council (CNR) and the European project FREECATS (NMP3-SL-2012-280658). The COST Action CM1302 “European Network on Smart Inorganic Polymers” (SIPs) (<http://www.sips-cost.org/home/index.html>) is also acknowledged.

Notes and references

Consiglio Nazionale delle Ricerche, Istituto di Chimica dei Composti Organometallici (ICCOM-CNR), Via Madonna del Piano 10, 50019 Sesto Fiorentino (Firenze), Italy. a.rossin@iccom.cnr.it

TOC Graphic

This Highlight describes the crystal structures and network topology of thiazole and thiazolidine-containing MOFs and CPs, along with their applications in the fields of CO₂ adsorption, luminescence, magnetism and heterogeneous catalysis.



Biography



Andrea Rossin was born in Biella, Northern Italy, in 1974. In 2004 he received his Ph.D. in Chemistry from Cardiff University (Wales, UK). After a post-doctoral training at the UAB (Barcelona, Spain) in 2005, he moved to Florence to join the the Institute of Chemistry of OrganoMetallic Compounds (ICCOM-CNR) in 2006. He is a permanent Reseacher since 2010. His research interests are manifold: Metal-Organic Frameworks and Coordination Polymers synthesis and characterization, along with their applications in H₂/CO₂ adsorption and heterogeneous catalysis; reactivity studies of ammonia-borane and amino-boranes as chemical hydrogen storage materials with transition metal organometallics; synthesis and reactivity studies of transition metal hydrides.



Giuliano Giambastiani received his Ph.D. in Chemistry from the University of Florence (Italy) and the University of Pierre et Marie curie – Paris IV (France) in 2000. After spending a period as Premier Assistant à la Faculté des Sciences at the EPFL in Lausanne he joined the Institute of Chemistry of OrganoMetallic Compounds where he is Senior Researcher since 2007. His current scientific activity spans from organic and organometallic synthesis and catalysis (homogeneous and heterogeneous) to the preparation and characterization of technologically advanced materials and composites based on functionalized carbon nanostructures such as carbon nanotubes, graphene, graphene-oxide and fullerenes.

- 1 K. Byrappa and M. Yoshimura, *Handbook of Hydrothermal Technology: A Technology for Crystal Growth and Materials Processing*, Noyes Publications (NY), 2001.
- 2 (a) H. Li, M. Eddaoudi, M. O'Keeffe and O. M. Yaghi, *Nature* 1999, **402**, 276-279. (b) N. L. Rosi, J. Eckert, M. Eddaoudi, D. T. Vodak, J. Kim, M. O'Keeffe and O. M. Yaghi, *Science* 2003, **300**, 1127.
- 3 J. H. Cavka, S. Jakobsen, U. Olsbye, N. Guillou, C. Lamberti, S. Bordiga and K. P. Lillerud, *J. Am. Chem. Soc.* 2008, **130**, 13850-13851.
- 4 (a) A. Dhakishnamoorthy, E. Garcia, *Chem. Soc. Rev.* 2012, **41**, 5262-5284. (b) M. Yoon, R. Srirambalaji and K. Kim, *Chem. Rev.* 2012, **112**, 1196-1231. (c) K. P. Lillerud, U. Olsbye and M. Tilset, *Top. Catal.* 2010, **53**, 859-868.
- 5 (a) L. E. Kreno, K. Leong, O. K. Farha, M. Allendorf, R. P. Van Duyne and J. T. Hupp, *Chem. Rev.* 2012, **112**, 1105-1125. (b) O. Shekhah, J. Liu, R. A. Fischer and C. Woll, *Chem. Soc. Rev.* 2011, **40**, 1081-1106.
- 6 (a) C. M. Doherty, D. Buso, A. J. Hill, S. Furukawa, S. Kitagawa and P. Falcaro, *Acc. Chem. Res.* 2014, **47**, 396-405. (b) R. Ricco, L. Malfatti, M. Takahashi, A. J. Hill and P. Falcaro, *J. Mater. Chem. A* 2013, **1**, 13033-13045. (c) E. Coronado and G. M. Espallargas, *Chem. Soc. Rev.* 2013, **42**, 1525-1539.
- 7 (a) J.-R. Li, J. Sculley and H.-C. Zhou, *Chem. Rev.* 2012, **112**, 869-932. (b) J.-R. Li, R. J. Kuppler and H.-C. Zhou, *Chem. Soc. Rev.* 2009, **38**, 1477-1504.
- 8 (a) A. Y. Robin, K. M. Fromm, *Coord. Chem. Rev.* 2006, **250**, 2127-2157. (b) C. Janiak, *Dalton Trans.* 2003, 2781-2804.
- 9 T. Lescouet, E. Kockrick, G. Bergeret, M. Pera-Titus, S. Aguado and D. Farrusseng, *J. Mater. Chem.* 2012, **22**, 10287-10293.
- 10 K. Koh, A. G. Wong Foy and A. J. Matzger, *Angew. Chem. Int. Ed.* 2008, **47**, 677-680.
- 11 (a) G. Tuci, A. Rossin, X. Xu, M. Ranocchiari, J. A. Van Bokhoven, L. Luconi, I. Manet, M. Melucci and G. Giambastiani, *Chem. Mater.* 2013, **25**, 2297-2308. (b) M. Servalli, M. Ranocchiari, J. A. Van Bokhoven, *Chem. Commun.* 2012, **48**, 1904-1906.
- 12 M.-L. Tong, X.-M. Chen, X.-L. Yu and T. C. W. Mak, *J. Chem. Soc., Dalton Trans.* 1998, 5-6.
- 13 M. Rivera-Carrillo, I. Chakraborty and R. G. Raptis, *Cryst. Growth Des.* 2010, **10**, 2606-2612.
- 14 S. T. Zheng, Y. Li, T. Wu, R. A. Nieto, P. Feng and X. Bu, *Chem.-Eur. J.* 2010, **16**, 13035-13040.
- 15 S. Soo Han and W. A. Goddard III, *J. Am. Chem. Soc.* 2007, **129**, 8422-8423.
- 16 (a) M. Higuchi, K. Nakamura, S. Horike, Y. Hijikata, N. Yanai, T. Fukushima, J. Kim, K. Kato, M. Takata, D. Watanabe, S. Oshima and S. Kitagawa, *Angew. Chem. Int. Ed.* 2012, **51**, 8369-8372. (b) K. L. Mulfort and J. T. Hupp, *J. Am. Chem. Soc.* 2007, **129**, 9604-9605.
- 17 (a) C. I. C. Esteves, A. M. F. Silva, M. M. M. Raposo and S. P. G. Costa, *Tetrahedron* 2009, **65**, 9373-9377. (b) R. M. F. Batista, S. P. G. Costa and M. M. M. Raposo, *Tetrahedron Lett.* 2004, **45**, 2825-2828.
- 18 (a) S.-H. Lee, A. Otomo, T. Nakahama, T. Yamada, T. Kamikado, S. Yokoyama, S. Mashiko, *J. Mater. Chem.* 2002, **12**, 2187-2188. (b) E. M. Breitung, C.-F. Shu, R. J. McMahon, *J. Am. Chem. Soc.* 2000, **122**, 1154-1160.
- 19 B. Di Credico, G. Reginato, L. Gonsalvi, M. Peruzzini and A. Rossin, *Tetrahedron* 2011, **67**, 267-274.
- 20 For a detailed description of the chemico-physical properties and synthetic procedures of N,S-containing heterocycles see: *Chemistry of Heterocyclic Compounds: Thiazole and Its Derivatives, Part One, Volume 34*. Ed. J. V. Metzger, John Wiley & Sons Inc. (1979).
- 21 (a) M. James and J. Horvat, *J. Phys. Chem. Solids* 2002, **63**, 657-663. (b) M. James, *J. Chem. Soc., Dalton Trans.* 1998, 2757-2760. (c) M. James, H. Kawaguchi and K. Tatsumi, *Polyhedron* 1998, **17**, 1843-1850.
- 22 V. A. Blatov, *Struct. Chem.* **2012**, **23**, 955-963. <http://www.topos.ssu.samara.ru>.
- 23 A. Rossin, G. Tuci, G. Giambastiani and M. Peruzzini, *ChemPlusChem* 2014, **79**, 406-412.
- 24 S. W. Suh, C.-H. Kim and I. H. Kim, *Acta Cryst.* 2007, **E63**, m2177.
- 25 E.-C. Wang, J. Li, Y.-L. Li, E.-C. Yang and X.-J. Zhao, *Synth. React. Inorg. Met.* 2011, **41**, 791-797.
- 26 D. Gao, X. Fang, K.-K. Zhang, L.-M. Cai and J.-D. Wang, *Acta Cryst.* 2012, **E68**, m641-m642.
- 27 B.-X. Liu, H.-Q. Ge and D.-J. Xu, *Acta Cryst.* 2006, **E62**, m1439-m1441.
- 28 J. Abedini, A. Morsali, R. Kempe and I. Hertle, *J. Coord. Chem.* 2005, **58**, 1719-1726.
- 29 (a) A. Abedi and F. Rezaei, *Acta Cryst.* 2011, **E67**, m886. (b) B. Notash, N. Safari, A. Abedi, V. Amani and H. R. Khavasi, *J. Coord. Chem.* 2009, **62**, 1638-1649.
- 30 Indeed, discrete (0D) metal complexes have been obtained with thiazole-2-carboxylic acid, thiazole-4-carboxylic acid and thiazole-2,4-dicarboxylic acid when combined with 3d metal ions (Cu^{II}, Zn^{II}, Co^{II}). See reference [19] and: A. Rossin, B. Di Credico, G. Giambastiani, L. Gonsalvi, M. Peruzzini and G. Reginato, *Eur. J. Inorg. Chem.* 2011, 539-548. The same chelating coordination mode

- has also been observed in the case of 2-amino-5-thiazoleacetic acid (forming a six-membered ring): K. A. Siddiqui, G. K. Mehrotra and R. L. LaDuca, *Polyhedron* 2009, **28**, 4077-4083.
- 31 A. Aprea, V. Colombo, S. Galli, N. Masciocchi, A. Maspero, G. Palmisano, *Solid State Sci.* 2010, **12**, 795-802.
- 32 Y.-F. Yue, E.-Q. Gao, C.-J. Fang, T. Zheng, J. Liang and C.-H. Yan, *CrystEngComm* 2008, **10**, 614-622.
- 33 H.-H. Lin, S. Mohanta, C.-J. Lee and H.-H. Wei, *Inorg. Chem.* 2003, **42**, 1584-1589.
- 34 H.-M. Liu, W. Zhang, Y. Zheng and W.-Q. Zhang, *J. Mol. Struct.* 2004, **698**, 37-40.
- 35 O. R. Evans and W. Lin, *J. Chem. Soc., Dalton Trans.* 2000, 3949-3954.
- 36 C.-Y. Su, M. D. Smith, A. M. Goforth and H.-C. zur Loye, *Inorg. Chem.* 2004, **43**, 6881-6883.
- 37 J. M. Ellsworth, C.-Y. Su, Z. Khaliq, R. E. Hipp, A. M. Goforth, M. D. Smith and H.-C. Zur Loye, *J. Mol. Struct.* 2006, **796**, 86-94.
- 38 J. M. Ellsworth, Z. M. Khaliq, M. D. Smith and H.-C. Zur Loye, *Solid State Sci.* 2008, **10**, 825-836.
- 39 R. C. Severance, A. M. Patel, M. D. Smith and H.-C. Zur Loye, *J. Chem. Crystallogr.* 2012, **42**, 258-262.
- 40 X. Zhou, Z. Zhang, B. Li, F. Yang, Y. Peng, G. Li, Z. Shi, S. Feng and J. Li, *New J. Chem.* 2013, **37**, 425-430.
- 41 X.-D. Chen, H.-F. Wu, X.-H. Zhao, X.-J. Zhao and M. Du, *Cryst. Growth Des.* 2007, **7**, 124-131.
- 42 X.-Y. Wei, W. Chu, R.-D. Huang, S.-W. Zhang, H. Li and Q.-L. Zhu, *Inorg. Chem. Commun.* 2006, **6**, 1161-1164.
- 43 L. Dong, W. Chu, Q. Zhu and R. Huang, *Cryst. Growth Des.* 2011, **11**, 93-99.
- 44 (a) Y.-Y. Yin, X.-Y. Chen, X.-C. Cao, W. Shi and P. Cheng, *Chem. Commun.* 2012, **48**, 705-707. (b) A. Rossin, B. Di Credico, G. Giambastiani, M. Peruzzini, G. Pescitelli, G. Reginato, E. Borfecchia, D. Gianolio, C. Lamberti and S. Bordiga, *J. Mater. Chem.* 2012, **22**, 10335-10344.
- 45 Y.-Y. Yin, J.-G. Ma, Z. Niu, X.-C. Cao, W. Shi and P. Cheng, *Inorg. Chem.* 2012, **51**, 4784-4790.
- 46 G. Tuci, G. Giambastiani, S. Kwon, P. C. Stair, R. Q. Snurr and A. Rossin, *ACS Catal.* 2014, **4**, 1032-1039.